Science of the Total Environment 685 (2019) 1097–1106

Contents lists available at ScienceDirect

Science of the Total Environment

journal homepage: www.elsevier.com/locate/scitotenv

Mechanical formation of micro- and nano-plastic materials for environmental studies in agricultural ecosystems

A.F. Astner [a], D.G. Hayes [a,*], H. O'Neill [b], B.R. Evans [b], S.V. Pingali [b], V.S. Urban [b], T.M. Young [c]

[a] The University of Tennessee, Biosystems Engineering and Soil Science, 2506 E J. Chapman Dr, Knoxville, TN 37996, United States of America
[b] Oak Ridge National Laboratory, 1 Bethel Valley Road, Oak Ridge, TN 37831, United States of America
[c] The University of Tennessee, Center for Renewable Carbon, 2506 Jacob Dr, Knoxville, TN 37996, United States of America

HIGHLIGHTS

- Micro- (MPs) and nanoplastics (NPs) prepared from agricultural plastics
- Cryogenics, milling and sieving used to prepare MPs; wet grinding to prepare NPs
- MP fractions: 840 μm, 250 μm, 100 μm, and 45 μm; NPs: 360–390 nm
- Size reduction procedure did not produce any artifacts in chemical structure.
- MPs and NPs are useful for fundamental research in agricultural soils.

GRAPHICAL ABSTRACT

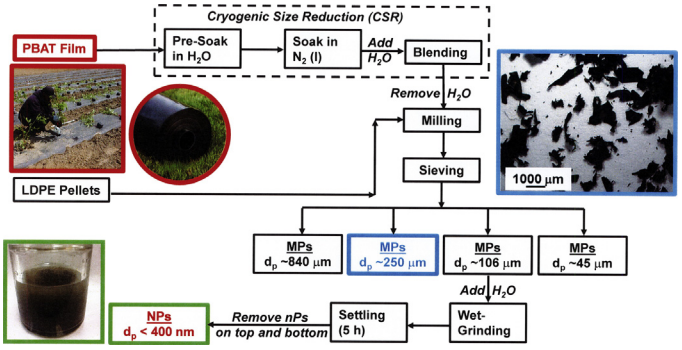

ARTICLE INFO

Article history:
Received 22 March 2019
Received in revised form 10 June 2019
Accepted 15 June 2019
Available online 17 June 2019

Editor: Jay Gan

Keywords:
Agricultural soils
Low-density polyethylene (LDPE)
Microplastics
Nanoplastics
Polybutylene adipate-*co*-terephthalate (PBAT)
Terrestrial ecosystems

ABSTRACT

Release of microplastics (MPs) and nanoplastics (NPs) into agricultural fields is of great concern due to their reported ecotoxicity to organisms that provide beneficial service to the soil such as earthworms, and the potential ability of MPs and NPs to enter the food chain. Most fundamental studies of the fate and transport of plastic particulates in terrestrial environments employ idealized MP materials as models, such as monodisperse polystyrene spheres. In contrast, plastics that reside in agricultural soils consist of polydisperse fragments resulting from degraded films employed in agriculture. There exists a need for more representative materials in fundamental studies of the fate, transport, and ecotoxicity of MPs and NPs in soil ecosystems. The objective of this study was therefore to develop a procedure to produce MPs and NPs from agricultural plastics (a mulch film prepared biodegradable polymer polybutyrate adipate-*co*-terephthalate (PBAT) and low-density PE [LDPE]), and to characterize the resultant materials. Soaking of PBAT films under cryogenic conditions promoted embrittlement, similar to what occurs through environmental weathering. LDPE and cryogenically-treated PBAT underwent mechanical milling followed by sieve fractionation into MP fractions of 840 μm, 250 μm, 106 μm, and 45 μm. The 106 μm fraction was subjected to wet grinding to produce NPs of average particle size 366.0 nm and 389.4 nm for PBAT and LDPE, respectively. A two-parameter Weibull model described the MPs' particle size distributions, while NPs

Abbreviations: AIC, Akaike's information criterion (used to assess the quality of the Weibull model to the fitting of particle size distribution data); BIC, Bayesian information criterion (used to assess the quality of the Weibull model to the fitting of particle size distribution data); DSC, differential scanning calorimetry; DLS, dynamic light scattering; d_p, average particle size (diameter); DTG, differential thermogram (DSC analysis); FTIR, Fourier transform infrared spectroscopy; GPC, gel permeation chromatography; LDPE, low-density polyethylene; M_n, number-averaged molecular weight; MP, microplastic; M_w, weight-averaged molecular weight; NP, nanoplastic; PBAT, polybutylene adipate-co-terephthalate; PDI, polydispersity index (for molecular weight); TGA, thermogravimetric analysis; X_c, mole fraction of crystalline morphology for PBAT and LDPE, Eq. (S1); α, scale parameter for the two-parameter Weibull model, Eq. (1); β, shape parameter for the two-parameter Weibull model, Eq. (1).

* Corresponding author.
E-mail address: dhayes1@utk.edu (D.G. Hayes).

https://doi.org/10.1016/j.scitotenv.2019.06.241

possessed bimodal distributions. Size reduction did not produce any changes in the chemical properties of the plastics, except for slight depolymerization and an increase of crystallinity resulting from cryogenic treatment. This study suggests that MPs form from cutting and high-impact mechanical degradation as would occur during the tillage into soil, and that NPs form from the MP fragments in regions of relative weakness that possess lower molecular weight polymers and crystallinity.

1. Introduction

The rapid increase of global plastic production (322 million tons; 5% annual growth), combined with minimal recycling and improper disposal has led to increased release of post-consumer plastics into the environment (e.g., 250 million metric tonnes of plastic in the oceans projected for 2025, equivalent to 5.25 trillion plastic particles) (Alimi et al., 2018; Jambeck et al., 2015; Mattsson et al., 2015; Wright and Kelly, 2017). The plastic materials, originally macro- or meso-plastics (average particle size [diameter], or d_p, of >25 mm and 5–25 mm, respectively) undergo size reduction due to shear, chemical and biochemical reactions, resulting in defragmentation into micro- and nanoplastics (MPs and NPs, respectively) to produce d_p of 0.1–5000 μm and 1–1000 nm, respectively (Alimi et al., 2018; Gigault et al., 2018; Hartmann et al., 2019). (A thorough discussion on the defining size range for NPs is given in (Gigault et al., 2018).) Plastic litter accumulates in various environments, including marine (Alimi et al., 2018) and terrestrial (Horton et al., 2017; Nizzetto et al., 2016; Scheurer and Bigalke, 2018) habitats. The small plastic fragments exhibit major environmental health concerns impacting marine and terrestrial environment, either directly or as carriers of pesticides, plasticizers, or other potentially harmful agents (Bouwmeester et al., 2015; Koelmans et al., 2013). Most studies of ecotoxicity formation and behavior of MPs and NPs have been reported for marine environments, showing potential harm to microorganisms (Eckert et al., 2018; McCormick et al., 2014) (including the microbiome of macroorganisms (Lu et al., 2018; Oberbeckmann et al., 2018; Zhu et al., 2018)), fish, and other macroorganisms (Alimi et al., 2018; Bouwmeester et al., 2015; Horton et al., 2017; Mattsson et al., 2015). Recent studies have detected MPs in humans and other mammals, resulting from accumulation in the food chain (Bouwmeester et al., 2015; EFSA Panel on Contaminants in the Food Chain, 2016; Lu et al., 2018; Schwabl et al., 2018; Wright and Kelly, 2017).

In contrast, terrestrial MPs have been investigated only to a minimal extent, despite their presence at higher amounts compared to marine plastics (Alimi et al., 2018; Bläsing and Amelung, 2018; Horton et al., 2017; Nizzetto et al., 2016), and the detection of terrestrial NPs has not been reported in the literature to the best of our knowledge (although they are likely to occur (Ng et al., 2018)). Recent studies reported that MPs harm soil-dwelling organisms: earthworms, collembolans (hexapods) and microorganisms (Huerta Lwanga et al., 2017; Zhu et al., 2018).

The occurrence MPs and NPs on farmland is of particular concern, due to the potential harm to cropping and animal systems, which could lead to loss of agricultural productivity or accumulation of MPs and NPs in foods (Nizzetto et al., 2016). A major source of terrestrial plastic fragments are agricultural plastics, employed as coverings for high tunnels, silage film, drip tape, seed casings, plant trays and bags, and row covers (Hussain and Hamid, 2003; Scarascia-Mugnozza et al., 2011). The most extensive application of agricultural plastics is mulch film (Steinmetz et al., 2016), used in the production of vegetables and other specialty crops as covering on the soil to reduce weeds, control soil temperature, and prevent evaporative loss of soil moisture and erosion (Kasirajan and Ngouajio, 2012; Steinmetz et al., 2016). The global market for agricultural plastic films was 4 million tons ($10.6 million) in 2016, and is projected to grow at a rate of 5.6% per year through 2030 (von Moos et al., 2012).

Polyethylene (PE) is the most commonly used polymer for mulch films and other agricultural plastics (Hussain and Hamid, 2003; Kasirajan and Ngouajio, 2012; Scarascia-Mugnozza et al., 2011). Opportunities for recycling of agricultural plastics are minimal, and labor costs to retrieve plastic mulches after crop harvest are prohibitive to farmers (Kasirajan and Ngouajio, 2012; Miles et al., 2017). Often, agricultural plastics are stockpiled on farms for a long duration, providing the opportunity for fragmentation. Furthermore, agricultural plastics become embrittled due to environmental weathering during their service life, with ultraviolet radiation being the most significant factor (Hayes et al., 2017). Therefore, hand-retrieval of plastics would likely not remove all plastic fragments, resulting in the dispersal of the plastics into soil and watersheds. In addition, PE is poorly biodegradable, allowing for its long-term retention in the environment (de Souza Machado et al., 2017; Kasirajan and Ngouajio, 2012; Nizzetto et al., 2016; Steinmetz et al., 2016). In summary, improper disposal of agricultural plastics, exacerbated by embrittlement via environmental weathering, leads to the dispersal of the plastic fragments into agricultural soils.

To address the problems associated with PE mulch, biodegradable plastic mulches (BDMs) have been developed. These films, containing biodegradable polymeric blends that mimic the desirable mechanical properties of PE (e.g., high tensile stress and elongation, as possessed by blends enriched in polybutyrate, i.e., polybutylene adipate-*co*-terephthalate [PBAT]), are designed to be plowed into the field after the harvesting of the crop, where they should be fully biodegraded by soil-borne microorganisms into CO_2 and water within a ~2-year period (Hayes et al., 2019; Kasirajan and Ngouajio, 2012; Steinmetz et al., 2016). Therefore, since the biodegradation rate in soil is slow, MPs and NPs may reside in the soil for several months, and we have detected MPs from BDMs in soil at 20–40 kg/ha (M. English and S.M. Schaeffer, personal communication).

Fundamental studies are required to understand the behavior, fate and transport of MPs and NPs in terrestrial environments as well as for ecotoxicity and adsorption of toxicants such as pesticides and plasticizers. Such studies should employ representative MP and NP models. Yet, most investigations have employed overly simplified or non-representative MP and NP materials such as monodisperse polystyrene spheres (Gigault et al., 2018). The absence of appropriate model MPs and NPs for terrestrial environments motivated the authors to prepare such models from agricultural plastics.

The methodology developed includes cryogenic soaking (to simulate embrittlement that typically occurs through environmental weathering (Hayes et al., 2017)), milling and sieve fractionation (to prepare different MP subpopulations and to simulate cutting and high-impact mechanical degradation, as would occur during tillage of plastics into the soil), followed by wet grinding (to prepare NPs) (Fig. 1). Mild operating conditions of milling and wet grinding were chosen (e.g., minimization of residence time to reduce friction-induced thermodegradation) so that artifacts in the chemical nature of the polymers such as oxidation or cross-linking would not occur.

Exposure to cryogenic conditions followed by mechanical milling is well known to induce size reduction of polymeric materials (Dümichen et al., 2015; Goedecke et al., 2017; Jonna and Lyons, 2005; Poulose et al., 2016; Robotti et al., 2016; Saba et al., 2015). A few recent studies have employed milling procedure to prepare model MPs from several different polymeric materials (e.g., polystyrene, polypropylene, PE and PBAT) for environmental research (Corradini et al., 2019;

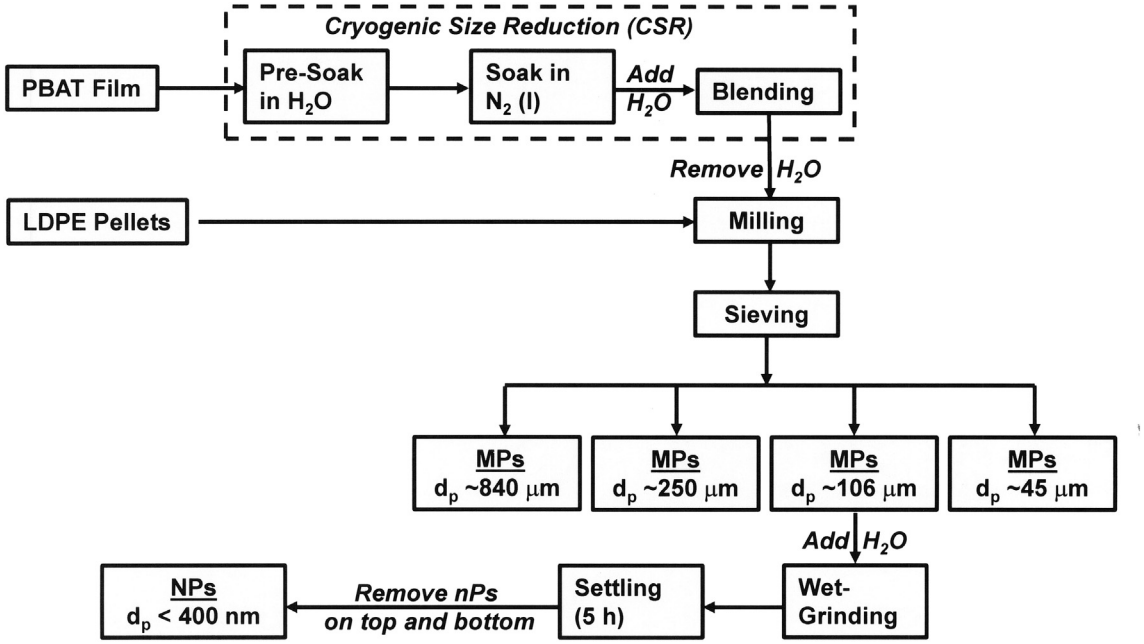

Fig. 1. Flow diagram for processing of micro- and nanoplastics (MPs and NPs, respectively).

Eitzen et al., 2019; Guo et al., 2018; Kühn et al., 2018; Xu et al., 2018; Zuo et al., 2019). The majority of these studies produced MPs of size >200 μm. Guo et al., (2018) prepared MPs of PE, polypropylene, polystyrene and polyvinylchloride of size ~10–40 μm, but used harsher mechanical grinding conditions that may have produced thermal degradation. Eitzen et al., (2019) performed a similar low-temperature milling and sieving approach to that employed herein, and obtained MP of sizes 5–100 μm. However, the cited study employed polystyrene, an inherently brittle polymer that possesses lower impact strength than the polymeric materials employed herein, and is not commonly employed in agriculture. The current study probes deeper than the previous studies in terms of the size distribution and physicochemical-related properties.

A unique aspect of this paper is the preparation of NPs from the MPs via wet grinding. Wet grinding is frequently employed to induce size reduction to the nanoscale (Elkharraz et al., 2003; Ravishankar et al., 2018; Schmidt et al., 2012; Schmidt et al., 2017; Watano et al., 2015; Wilczek et al., 2004; Zhang et al., 2018). Wet grinding is believed to better simulate the low-energy degradation of plastics in the environment than milling (Ravishankar et al., 2018). To the authors' knowledge, there are no commercially available sources of environmentally-relevant NPs other than monodisperse polystyrene spheres employed to calibrate laser light scattering and related techniques.

The objective of this study is therefore to develop a procedure that produces MPs and NPs from agricultural plastics (a mulch film composed of biodegradable polymer polybutyrate adipate-*co*-terephthalate (PBAT) and low-density PE [LDPE]), and to characterize the resultant materials in terms of size, size distribution and physicochemical properties. The methodology developed herein may also be useful to better understand the size reduction processes that occurs in nature, from mesoplastics to MPs (as would occur during plastics' tillage into the soil) and from MPs to NPs (as would simulate the low-impact shear events such as MP-soil collisions).

2. Experimental

2.1. Materials

BioAgri, a black-colored biodegradable mulch film prepared from Mater-Bi® (Grade EF04P), a starch-copolyester blend containing PBAT as its major constituent, was kindly provided by BioBag Americas (Dunevin, FL, USA). The film referred to as "PBAT" in this paper, possesses an apparent density of 22.81 ± 0.411 g m^{-2} thickness of 29 ± 1.2 μm, peak load of 12.05 ± 0.586 N and an elongation of 295 ± 30% at maximum tensile stress, in the machine direction (Hayes et al., 2017). Other physicochemical properties are given in the cited reference. The original film was provided as a 1.22 m-wide roll and stored at 20.6 ± 2.1 °C and 61.8 ± 10.6% relative humidity. LDPE beads, with a nominal diameter of 3 mm and particle density of 0.923 g cm^{-3}, were purchased from Dow Chemical (Midland, MI, USA). Chloroform (HPLC grade) was obtained from Fisher Scientific (Pittsburgh, PA, USA). Deionized water was used throughout all experiments.

2.2. Size reduction process to prepare MPs and NPs

Fig. 1 outlines the overall procedure employed to prepare MPs and NPs from PBAT and LDPE. Each of the process steps employed is described in detail below.

2.2.1. Cryogenic treatment of PBAT

PBAT films were cut with a paper cutter into strips with dimensions of ~120 mm (machine direction) x 20 mm (cross direction; Fig. S1). The fragments (~1.0 g) were presoaked in water (800 mL) for either 0, 5, or 10 min, recovered and transferred to a cryogenic container filled with liquid nitrogen (200 mL) and soaked for either 0, 5, or 10 min. The frozen PBAT film fragments (1.0 g) were transferred into an Osterizer type blender (Oster Accurate Blend 200, Boca Raton, FL, USA), and dry-comminuted for 10 s in order to break down the solidified glass-like structure of the plastic. Water (400 mL) was added to the PBAT fragments to form a slurry, and then the blender was operated at a fixed duration (5 or 10 min) at an angular velocity of 2 × 10^{-3} or 10 × 10^{-3} min^{-1}. After blending, the slurries were filtered under vacuum through a paper membrane filter (1 μm mesh) using a Büchner funnel apparatus. Solid PBAT particles (depicted in Fig. S1) were then air dried for 48 h to reduce moisture to <1%. A randomized experimental design was used to evaluate cryogenic processing conditions on d_p achieved.

2.2.2. Microplastic (MP) formation through milling and sieving

Cryogenic-treated PBAT fragments or untreated LDPE pellets (~1.0 g) were fed to a rotary mill (Model 3383-L10 Wiley Mini Mill, fitted with screen, Arthur H. Thomas Co., Philadelphia, PA, USA) by using sieve sizes of 20 mesh (840 μm) for the first pass and 60 mesh (250 μm) for the second pass through the mill. The residence time for milling was 20 min per pass. The MP particles recovered from milling (~1.0 g of PBAT or LDPE) were then fractionated via a cascade of four sieves (W.S. Tyler, Cleveland, OH, USA) with mesh sizes of #20 (840 μm), #60 (250 μm), #140 (106 μm), and #325 (45 μm) (Fig. 1). To enhance uniformity of the particle size distribution, the sieves were mounted on an Eppendorf thermomixer 5350 (Hamburg, Germany) and shaken for 30 min at 300 rpm. The % recovery for each sieving fractions was determined gravimetrically for three replicate experiments.

2.2.3. Nanoplastic (NP) formation through high-performance wet grinding

An aqueous slurry (4.0 L) containing 1.00 wt% of MPs was prepared, which underwent stirring for 24 h to allow for a homogenous distribution. For this process, the 106 μm-size MP-fraction was used rather than the to the smallest size MP fraction (45 μm) because the yield on the latter fraction was too small to provide sufficient amounts of material. After stirring, slurries were subjected to the wet-grinding process using a "supermass colloider" (MKCA6-2, Masuko Sangyo, Tokyo, Japan) at a speed of 1500 rpm and 27 subsequent passes (collection of particles and reintroduction into the colloider) to provide a uniform particle size reduction. The slurry recovered from wet-grinding was transferred to a 1000 mL beaker and magnetically stirred for 4 h (300 rpm at 25 °C). The resultant particles were dried at 40 °C for 48 h and are referred to as "NPs" herein. Analyses of NPs were conducted using aliquots collected from the middle height position of the slurry so that NPs flocculating at the top and settling at the bottom of the slurry were not included. The final concentration of the slurry aliquots were 0.37 (wt)% and 0.28% for PBAT and LDPE, respectively.

2.3. Particle size analysis

PBAT MPs formed via cryogenic treatment (Figs. 1 and S1) were scanned by a flatbed-scanner (MX 490 by Canon, Tokyo, Japan) and the particle dimensions were analyzed by ImageJ software (Schneider et al., 2012). PBAT and LDPE MPs belonging to each of the four MP sieve fractions identified in Fig. 1 were analyzed via stereomicroscopy and images were analyzed using ImageJ software. Examples of images produced by ImageJ vs. the corresponding stereomicrographs are presented in Fig. 2. The average MP diameter, d_p, was estimated using the Image J's "analyze particles" algorithm. The distribution of d_p derived from Image J analysis was fit by several different models using JMP® Pro 14.0 software (SAS Institute, Cary, NC, USA). The corrected Akaike's and Bayesian information criteria (AIC and BIC, respectively) were used to compare the quality of model fits. All statistical evaluations employed a significance level of $\alpha = 0.05$. The size and size distribution of NPs was determined using dynamic light scattering (DLS) at 25 °C. A detailed description of the procedures employed for determination of size distribution for MPs and NPs is given in the Supplementary Materials.

2.4. Chemical and thermal analyses of the original plastics, MPs and NPs

Chemical and thermal analyses were performed on the original polymeric materials, MPs (250 μm sieve fraction; Fig. 1), and NPs (produced after wet grinding) for both PBAT films and LDPE pellets. (For PBAT, samples were subjected to cryogenic treatment according to optimal conditions prior to milling and sieving). Analyses consisted of FTIR spectroscopy (chemical bonding properties), gel permeation chromatography (GPC; number- and weight-averaged molecular weight [M_n and M_w, respectively] and polydispersity index [*PDI*; M_w/M_n]), differential scanning calorimetry (DSC; thermal properties), and thermogravimetric analysis (TGA; thermal stability). The instrumentation and detailed procedures are given in the Supplementary Materials and are nearly

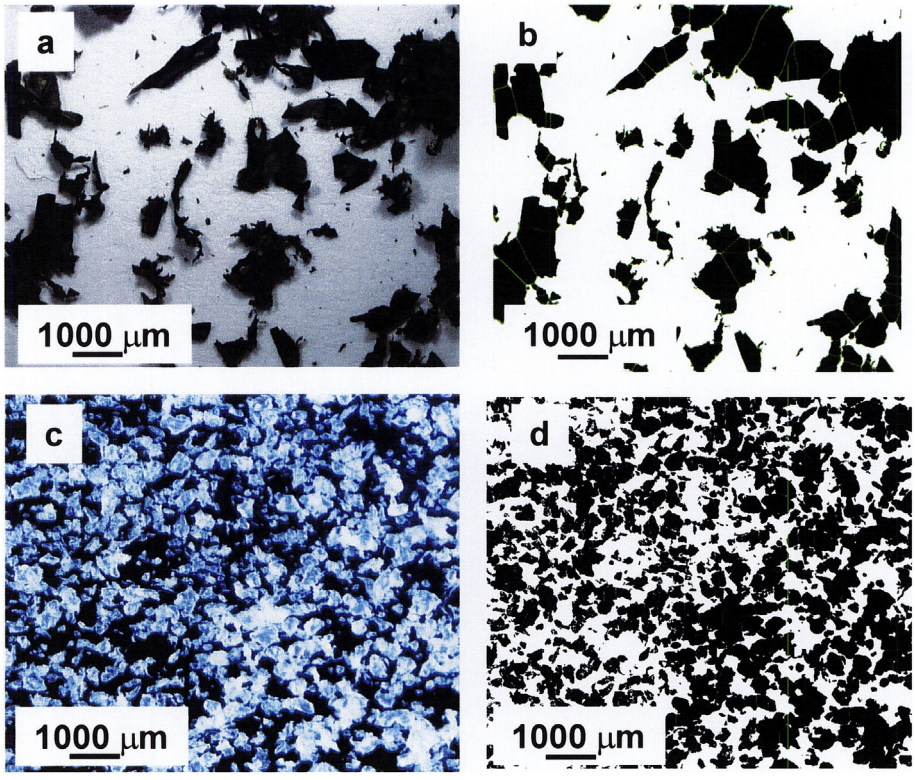

Fig. 2. Stereomicrographs of MPs (250 μm fraction resulting from milling followed by sieving; cf. Fig. 1): (a) PBAT and (c) LDPE, and (b) and (d) the corresponding images produced by Image J software. Prior to milling, PBAT film samples underwent cryogenic treatment according to the conditions of Run 4 of Table 1.

identical to those employed previously by the authors (Hayes et al., 2017).

3. Results and discussion

3.1. Effects of cryogenic treatment on the size reduction on PBAT mesoplastics

For efficient size reduction of a biodegradable agricultural mulch film (PBAT), cryogenic treatment was applied to induce embrittlement, leading to size reduction (Fig. S1). In the absence of cryogenic exposure, the PBAT film did not undergo size reduction upon mechanical milling (data not shown). A randomized design was used to evaluate the effect of cryogenic treatment processing conditions (duration of pre-soaking in water and soaking in liquid nitrogen, and the blending speed, time and presence vs. absence of water) for the minimization of d_p. Factor levels were selected based on observations from preliminary blending experiments performed with PBAT films, and accordingly, the experimental matrix was selected (Table 1). A more detailed analysis of the d_p distribution is given in Table S1. Results showed that increased severity of processing conditions significantly enhanced size reduction to d_p = 1–2 mm (Table 1, runs 4–6). Particularly, runs 4–6 shared the longest soaking time in liquid N_2 (10 min), indicating that it is the most influential factor for size reduction. Similarly, a recent study focusing upon polystyrene MPs found that the yield of MPs increased with residence time during a pre-cooling step (Eitzen et al., 2019). Blending time and speed were also influential factors, but to a lesser extent than soaking time.

Further evaluation of Table 1 data by prediction profiler statistical software confirmed the trends discussed above, that liquid nitrogen soaking time was the most influential factor, followed by blending time and speed (Fig. S2). Also, the statistical analysis demonstrated that no interaction within processing factors was observed, suggesting that increased levels for processing parameters will result in a more effective reduction of d_p (Fig. S2). The inclusion of water resulted in a well-blended mixture, leading to a slight reduction of d_p (Fig. S2). The software predicted that under optimal conditions, an average d_p value of 1.15 mm can be achieved (Fig. S2), which is slightly lower than the minimal value of d_p achieved, 1.43 mm (Table 1).

A representative histogram for d_p of PBAT MPs produced by cryogenic treatment is shown in Fig. 3, and histograms and particle counts for all runs of Table 1 are depicted in Figs. S3 and S4, respectively. The smallest size fraction of Fig. 3, 0–0.5 mm, served as the most prominent fraction, and as the average d_p for fractions increased, the population size slowly decreased. Several different size distribution models were evaluated for the quality of the fit to the data: log-logistic, Frechet, lognormal, and two-parameter Weibull. The latter distribution provided the best fit (followed by lognormal), exhibited by the lowest AIC and BIC values obtained for the fit. The two-parameter Weibull model is described by:

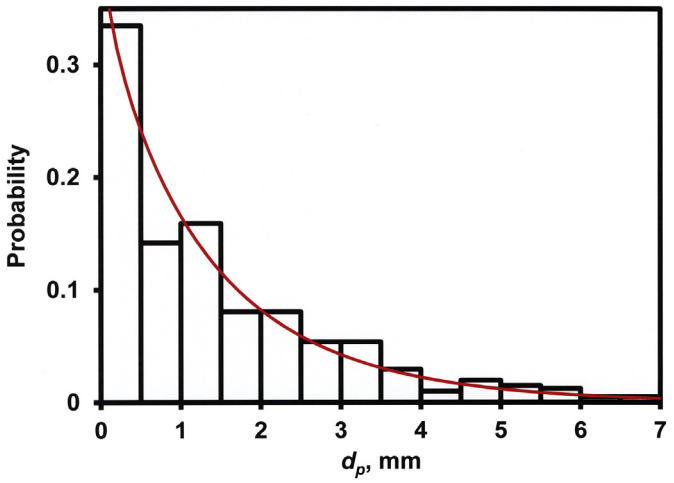

Fig. 3. Particle size distribution of PBAT MPs resulting from the cryogenic treatment represented by Run 4 of Table 1. The curve represents the fit of the two-parameter Weibull model (Eq. (1)) to the data.

$$f(x,\alpha,\beta) = \left\{ \frac{\beta}{\alpha}\left(\frac{x}{\alpha}\right)^{\beta-1} \exp\left(-\left[\frac{x}{\alpha}\right]^{\beta}\right) x \geq 00 x < 0 \right\} \quad (1)$$

where $\beta > 0$ is the shape parameter and $\alpha > 0$ is the scale parameter of the distribution. The two-parameter Weibull model is a flexible distribution model that is applied to a broad range of applications such as bioproduct development (Varga et al., 2001), terrestrial sediments (Allen et al., 2015), quality engineering for material strength data distribution (Young et al., 2015), two-phase materials in metallurgy (Fang et al., 1993; Lynch and Rowland, 2005), aerosols (Dunbar and Hickey, 2000), seed sizes (Domoradzki and Korpal, 2005), and wind speed distribution in aerodynamics (Seguro and Lambert, 2000). Of relevance to this study, the two-parameter Weibull model has also been demonstrated to be the most effective size distribution model to describe soil particles (Bayat et al., 2015; Esmaeelnejad et al., 2016).

The average d_p values obtained through the Weibull model fit, α and β values, and information on the quality of the fit (AIC and BIC) are given in Table 1. Run 4, which provided the lowest d_p, also experienced

Table 1
Effect of operational parameters for cryogenic size reduction of PBAT films on the average particle size for particles achieved (d_p) and the fitting of the particle size distribution by the two-parameter Weibull model.[a]

Run #	H_2O presoaking time, min	N_2 soaking time, min	Blending time, min	Blending speed, min^{-1} × 1000	d_p (measured), mm[b,c]	d_p (Weibull), mm	α[d]	β[d]	AIC[e]	BIC[f]
1	0	0	5	2	9.30 ± 4.53	9.29	8.71	0.878	2628	2636
2	0	5	5	2	3.17 ± 1.29	3.30	2.31	0.630	1621	1629
3	5	5	10	10	4.21 ± 1.54	4.19	4.53	1.300	1960	1968
4	5	10	10	10	1.47 ± 0.45	1.42	1.43	0.946	1132	1140
5	10	10	10	10	1.58 ± 0.63	1.58	1.53	0.931	1194	1202
6	10	10	5	2	1.68 ± 0.68	1.69	1.60	0.894	1239	1247
7	10	5	5	2	3.22 ± 1.47	3.22	3.28	1.051	1777	1785
8	5	5	5	10	3.64 ± 1.57	3.65	3.31	0.835	1856	1864

[a] Cryogenic treatment conditions: presoaking in H_2O (400 mL; except for Runs 1 and 2), followed by soaking in N_2 (200 mL) for cryogenic cooling, followed by blending of the resultant mesoplastics with water (400 mL), and then air-drying.
[b] Determined by ImageJ analysis of stereomicrographs from two images per sample.
[c] Error bars represent one standard deviation.
[d] Weibull model parameters (Eq. (1)).
[e] Akaike's information criterion.
[f] Bayesian information criterion.

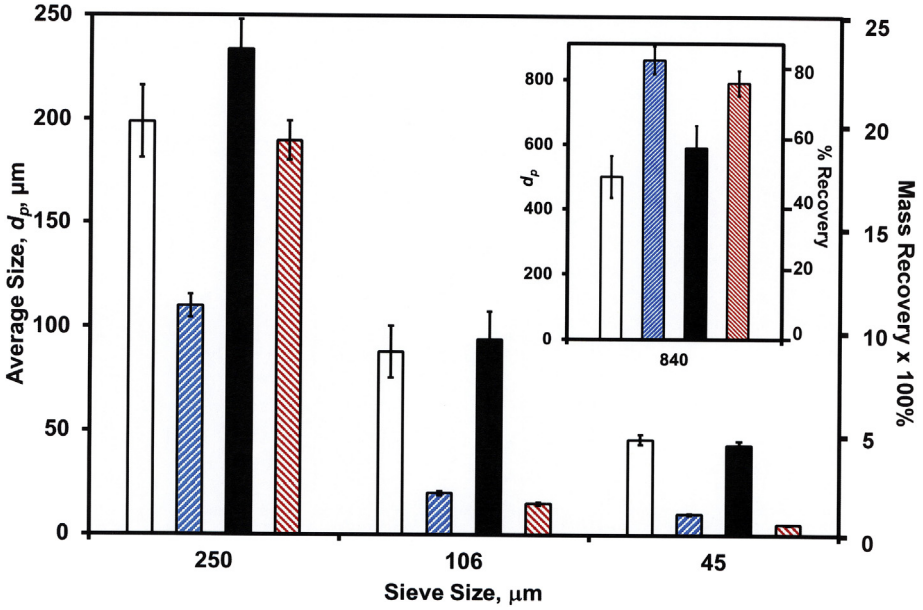

Fig. 4. Average particle size (d_p) and % recovery of mass for MPs of PBAT (unfilled and blue hatch [lower left to upper right], respectively) and LDPE (black solid filled and red hatch [lower right to upper left], respectively) obtained via dry milling (840 µm and 250 µm sieves for the first and second pass) of 1 g of feed, followed by sieving. Sieve sizes are indicated by solid black bars in the figures. d_p was determined by Image J analysis of stereomicrographs to fit the histogram for size distribution. Errors for d_p represent one standard deviation. LDPE particles were directly fed to the mill, while for PBAT, the feed was treated by cryogenic treatment according to optimal conditions (Run 4 of Table 1). The inset shows d_p and % recovery for the largest, 840 µm, sieve fraction.

the best fit of the two-parameter Weibull model to its size distribution data, evidenced by the minimization of AIC and BIC (Table 1). β values (~1.0) did not change appreciably with cryogenic conditions, and are reflective of a broad distribution with a maximum skewed toward the lower end of the distribution function (Table 1 and Fig. 3).

3.2. Effects of mechanical milling on MP formation

The use of mechanical milling led to the formation of PBAT and LDPE MPs that were isolated into four different sieving fractions (Fig. 1): 840 µm, 250 µm, 106 µm, and 45 µm (Fig. 4). More detailed information on

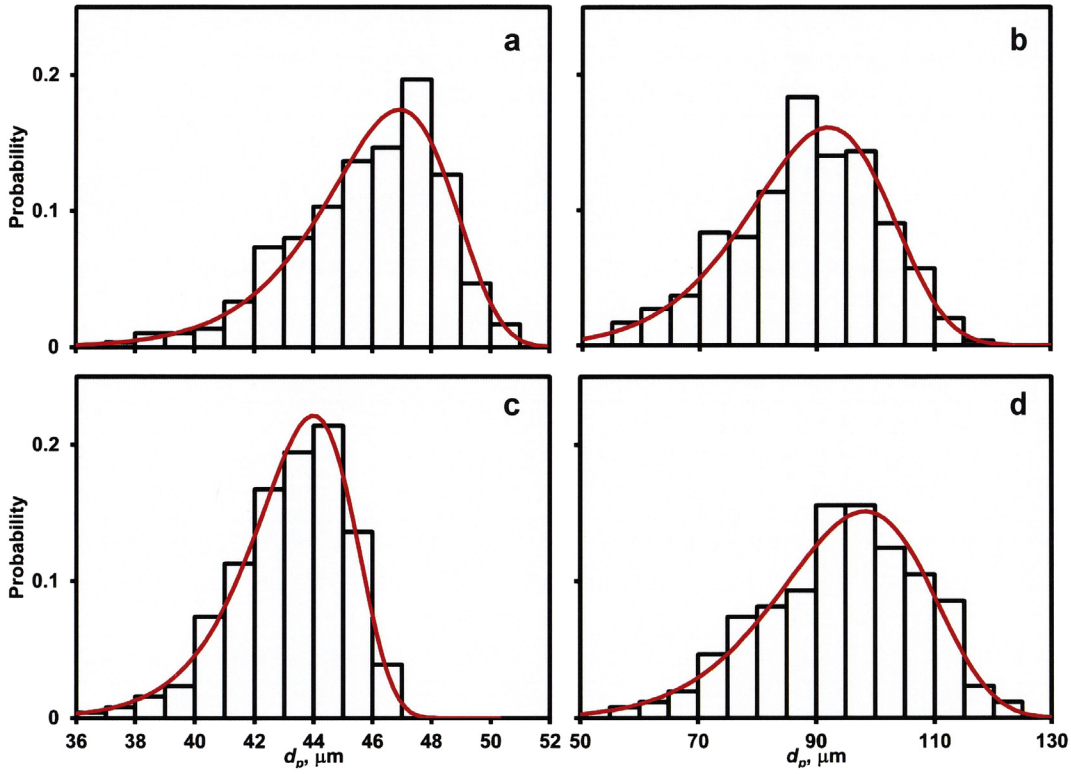

Fig. 5. Particle size distributions of (a, b) PBAT and (c, d) LDPE for the (a, c) 45 µm and (b, d) 106 µm nominal MP sieve fractions (after mechanical milling), with superimposed two-parameter Weibull model (Eq. (1)).

Table 2
Particle size distribution data for PBAT and LDPE MPs obtained via dry milling (840 μm and 250 μm sieves for the first and second pass) of 1 g of feed, followed by sieving, as determined by the Weibull model (Eq. (1))[a,b].

Polymer	Sieve fraction, μm	d_p (Weibull), μm	α	β	AIC	BIC
PBAT	840	500.7	527.2	9.58	3328	3335
	250	198.9	206.6	13.56	2553	2561
	106	88.1	93.4	8.18	2364	2372
	45	45.9	47.0	22.47	1375	1383
LDPE	840	591.0	619.7	10.58	2883	2890
	250	233.9	240.0	20.83	2062	2069
	106	94.2	99.8	8.23	2060	2067
	45	43.2	44.0	26.92	1058	1065

[a] Column headings described in Table 1.
[b] For PBAT, cryogenic exposure was employed per the conditions of Run 4 in Table 1.

the particle size distributions is given in Table S2. The mass recovery and d_p values for the two smallest sieve fractions, 106 μm and 45 μm, were nearly equal for both plastics with a mass recovery of 2 wt% and 1 wt %, respectively, and d_p values were nearly equal to the nominal sieve sizes (Fig. 4). For the 250 μm fraction, the recovery was lower for PBAT (11%) than for LDPE (18%), and d_p was lower for the former plastic (and less than the nominal size). These results reflect that mechanically milled PBAT contains a larger amount of coarser, less geometrically uniform, particles than milled LDPE, likely a result of PBAT being a softer and less dense polymeric material. The same trend serves as the underlying cause of the larger variability in d_p for PBAT for the 840 μm and 250 μm sieve fractions (Fig. 4). In summary, shear force via milling (supported by additional degradation via cryogenic treatment for PBAT) produced MPs at low-to-moderate yields.

Similar to PBAT MP particles obtained by cryogenic treatment, the size distribution of d_p was best fit by a two-parameter Weibull model for all MP sieve fractions produced by milling (Figs. 5 and S5). Parameters related to the fit of the Weibull model are given in Table 2, while particle count vs. d_p is depicted in Fig. S6. The fit of the Weibull model improved as the sieve size of the fractions decreased, noted by a decrease of AIC and BIC (Table 2). Unlike the distribution obtained for cryogenic-treated MPs, which was skewed toward the lower end of the d_p distribution (i.e., $\beta \approx 1.0$; Table 1), for all sieve fractions, the distributions were slightly skewed in favor of higher d_p values ($\beta > 8$; Table 2). The narrowest size distribution occurred for the 45 μm MP sieve fractions and for LDPE fractions compared to PBAT fractions (i.e., highest β value), the latter trend reflecting coarser and less geometrically uniform particles for PBAT as discussed above. The production of NPs was not detected, noting that the smallest size sieve fraction, 45 μm, provided MP particles of size (d_p) ≥36 μm. Moreover, it is unlikely that mechanical tilling of plastic mulch films will directly produce NPs.

3.3. Effects of wet-grinding on NP formation from MPs

Wet grinding was applied to the 106 μm MPs fraction of both plastics to produce NPs, with d_p measured by DLS. Both materials yielded NPs

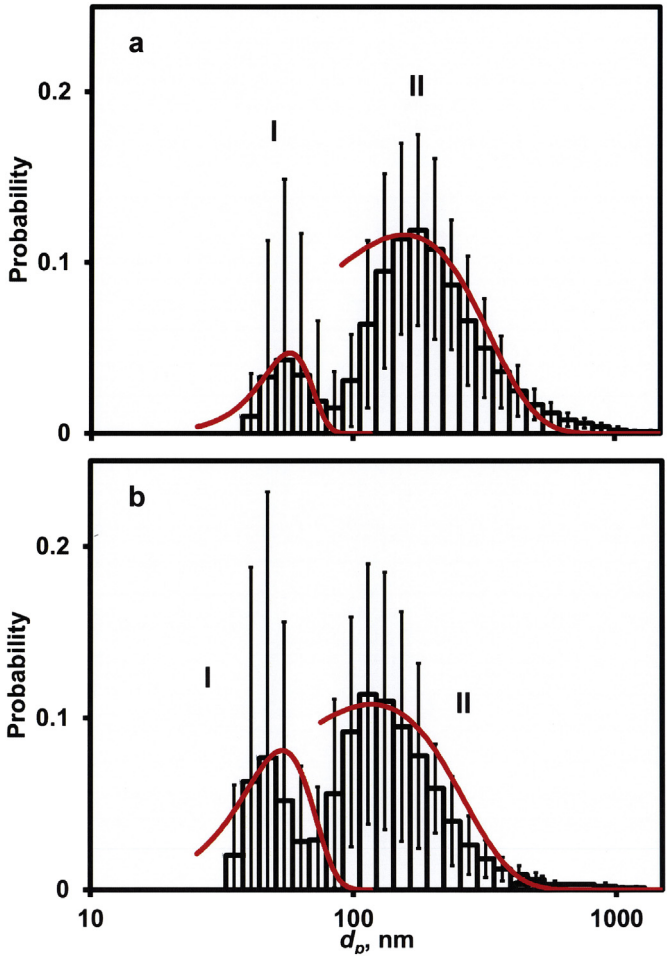

Fig. 6. Histograms of particle size (d_p,) for (a) PBAT and (b) LDPE NPs, formed from the wet-grinding treatment of the 106 μm- MP sieve fraction. Error bars represent ±one standard deviation of the dataset. Curves represent two-parameter Weibull model fits to size distribution fractions I and II, as listed in Table 3.

with similar bimodal distributions, with the major and minor fractions (I and II, respectively, with I being ~2.5-fold higher in intensity than II) possessing maxima at d_p values of ~500 nm and ~60 nm, respectively (Table 3 and Fig. 6). The size of fraction I is ~15-fold smaller than that of the initial 106 μm sieve fraction (Table 2 and Fig. 5b, d). Average d_p values for PBAT and LDPE NPs (i.e., both fractions combined) were 366.6 ± 6.5 nm and 389.4 ± 10.7 nm (error bars reflect standard deviation), respectively, and spanned the range ~40–1300 nm, with the range of LDPE being slightly broader (Fig. 6 and Table 3). These results suggest that degradation due to low shear may occur through two steps, one of which reduces size 15-fold and the other further reducing size by an additional factor of 10. For each fraction, lower d_p values were

Table 3
Size (d_p) and size distribution data for NPs of produced by wet-grinding of PBAT and LDPE MPs (106 μm sieve fraction) via Dynamic Light Scattering (DLS) analysis[a,b,c].

Polymer and fraction	PBAT, I	PBAT, II	PBAT, I + II	LDPE, I	LDPE, II	LDPE, I + II
d_p range, nm	37.7–91.3	91.3–1281	37.7–1281	32.7–91.3	91.3–1357	32.7–91.3
d_p (mean), nm[d]	63.8 ± 13.7	536.8 ± 151.8	366.0 ± 6.5	60.9 ± 17.8	485.7 ± 123.6	389.4 ± 10.7
α (Weibull), nm	59.8	243.0		58.3	190.5	
β (Weibull)	5.00	1.81		3.71	1.75	
AIC	129.5	1036		273.5	796.9	
BIC	130.0	1041		276.1	801.2	

[a] Size distributions and column headings described in Fig. 6.
[b] Row headings defined in Table 1.
[c] For PBAT, cryogenic exposure was employed per the conditions of Run 4 in Table 1.
[d] Error bars represent one standard deviation.

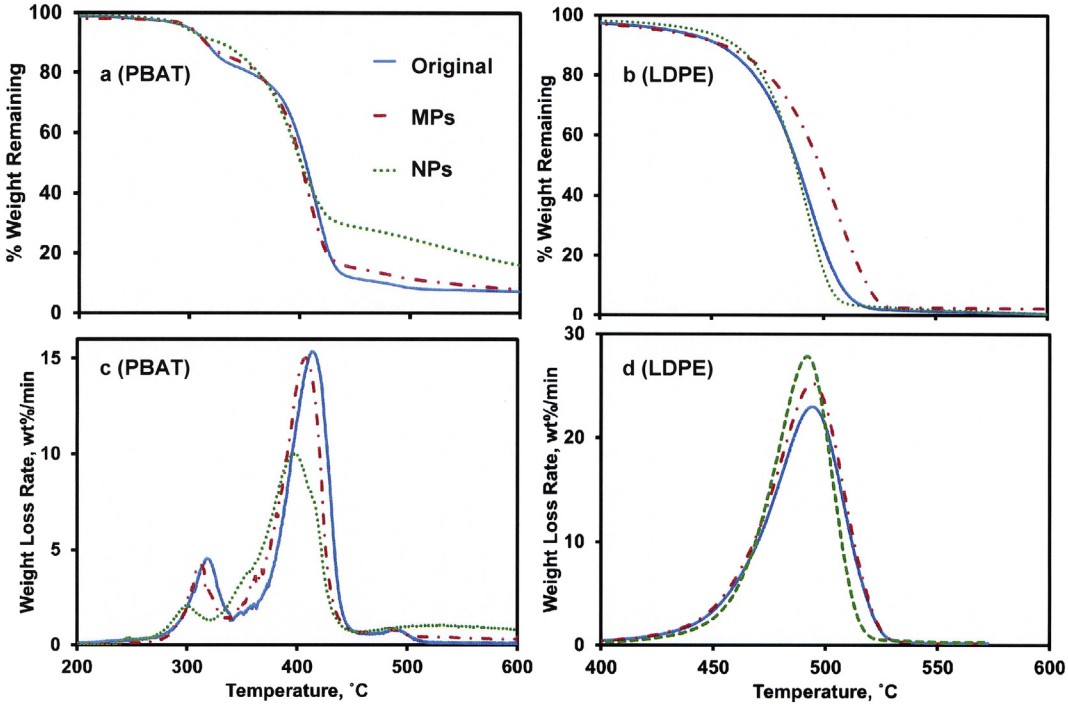

Fig. 7. (a, b) TGA and (c, d) DTG curves before processing initial polymer, after dry-milling (MPs) and wet grinding (NPs) of (a, c) PBAT and (b, d) LDPE. MPs consist of the 250 μm sieve fraction of dry milled plastics (cryogenic treatment applied to PBAT according to the optimal conditions: Run 4 of Table 1); NPs were produced via wet grinding of the 106 μm sieve fraction μPs after dry milling.

observed for LDPE, despite the original LDPE material possessing a higher d_p (Table 3 and Figs. 5 and 6). However, the aqueous solution of LDPE NPs produced by wet grinding contained a significant fraction of particles that flocculated on top that was not included in the sample analyzed by DLS. The flocculation is due to the density of LDPE being lower than that of water and the polymer's hydrophobicity. Another possible cause is the creeping of the NPs in the upward direction due to adhesion with the glass container walls, a phenomenon recently reported for polystyrene NPs (Eitzen et al., 2019). The same study reported that adhesion was lessened when the polystyrene NPs were oxidized by ozone (Eitzen et al., 2019). Environmentally-weathered PE is known to undergo oxidation, forming polar functional groups on its surface such as hydroxyls and carboxylates (Hayes et al., 2017). It is likely that the flocculation of NPs formed from weathered LDPE would be lessened. In contrast, PBAT NPs were evenly dispersed throughout the slurry, even in the absence of stirring.

The size distribution model that fit the two NP fractions for each polymeric material was the two-parameter Weibull model (Fig. 6). The smaller, ~60 nm –sized fractions (I) were narrower in the width of their size distributions than the larger size fraction (II), noted by the larger shape factor, β (Table 3), and both distributions were narrower than the original starting material, the 106 mm sieve fraction (Table 2). Future research is needed to better understand the relationship between wet grinding conditions and the resultant sizes and size distributions of the NP products.

3.4. Effect of size reduction on chemical and thermal properties of plastics

Chemical and thermal analyses of MPs and NPs were compared to the original plastic feedstock to determine if size reduction promoted any changes in properties. MP samples consisted of the 250 μm sieve fraction of dry milled plastics, while NPs were produced via wet grinding of the 106 μm MPs sieve fraction.

The thermal stability of MPs and NPs was examined by analysis of TGA curves (Fig. 7a, b) and differential thermograms (DTGs) (rate of heat loss vs. temperature; Fig. 7c, d). For the PBAT-rich film, the first major heating stage was found at temperatures between 300 °C and 318 °C, representing the decomposition of starch, while the second, largest, stage (~400 °C) represents the decomposition of PBAT (Hayes et al., 2017). The mass remaining at the maximum temperature, 600 °C, reflects minor components such as binders and fillers, and perhaps gels (Hayes et al., 2017). No weight loss was observed for temperatures <200 °C, suggesting the absence of water and volatiles. The formation of MPs led to a slight shifting of both major heating stages to lower temperatures (Fig. 7a, c). Upon further size reduction to NPs, the heating stages for starch and PBAT were shifted more significantly to lower temperatures. For LDPE, while TGA curves were nearly identical for the original material and MPs, the curve for NPs was slightly shifted to lower temperatures, to a much lesser extent than PBAT. (Fig. 7b, d).

The loss of thermostability by starch, PBAT and LDPE may be due to either a decrease of crystallinity or molecular weight. To address, crystallinity (X_c) was determined from the enthalpy of melting measured using DSC (discussed in the Supplementary Materials). For both polymeric materials, cryogenic exposure followed by mechanical milling increased X_c nearly two-fold, and NPs and MP possessed similar values (Table 4). An increase of crystallinity was also observed during

Table 4
Comparison of molecular weight-related and thermal properties of PBAT and LDPE plastics and the MPs and NPs derived from it[a,b].

Sample	M_n, kDa	M_w, kDa	*PDI*	X_c x100%[c]
PBAT, Original	89.7 ± 0.4	289 ± 15	3.22 ± 0.18	21.5 ± 0.6
PBAT, MP	98.0 ± 2.0	209 ± 6	2.13 ± 0.01	39.7 ± 0.9
PBAT, NP	110 ± 1.8	205 ± 2	1.87 ± 0.01	32.5 ± 0.7
LDPE, Original	*nd*	*nd*	*nd*	24.2 ± 0.2
LDPE, MP	*nd*	*nd*	*nd*	41.5 ± 0.5
LDPE, NP	*nd*	*nd*	*nd*	42.9 ± 0.4

[a] MPs consist of the 250 mm sieve fraction of dry milled PBAT, treated using cryogenic treatment under the conditions described in Run 4 of Table 1.
[b] NPs were produced via wet grinding of the 106 μm sieve fraction μPs after dry milling; Error bars represent one standard deviation of two sample measurements; *nd* = not determined.
[c] Crystallinity of PBAT, determined from the enthalpy of melting measured via DSC analysis, and calculated as described in detail in the Supplementary materials.

embrittlement caused by environmental weathering (Hayes et al., 2017), suggesting the underlying cause of the increase of X_c was cryogenic exposure. DSC analysis demonstrated that the melting and glass transition temperatures of PBAT and LDPE underwent slight changes (discussed in Supplementary Materials).

Therefore, the loss of thermostability is likely a result of depolymerization, a hypothesis supported by GPC analysis of PBAT. Depolymerization occurred slightly during the formation of MPs (i.e., cryogenic treatment followed by Wiley milling), noted by the 27.6% decrease of M_w; but, size reduction of MPs to NPs did not decrease M_w appreciably, 1.4% (Table 4). In contrast, the molecular weight distribution was narrower (i.e., PDI lower) and M_n slightly higher for MPs compared to the original polymeric film, and for NPs compared to MPs, suggesting the lower-molecular weight polymers were removed during milling and wet grinding (Table 4). These trends may reflect the selective degradation of local regions that are weaker in strength (e.g., amorphous morphological regions), where lower molecular weight polymers would be expected to reside. In contrast, smaller particles recovered from wet grinding of plastics typically undergo a slight decrease of M_n and M_w and a minor increase of PDI (Ravishankar et al., 2018). Herein, NP samples were taken from the middle layer of the slurry, such that smaller particles, which flocculated near the top layer, were less likely to have been contained in the sample.

TGA also provides the relative proportion of components, such as PBAT and starch. Size reduction to MPs decreased the starch content from 16.8% to 13.0%, and further size reduction to NPs further reduced the starch content to 8.3% (Fig. 7a, c). In contrast, the PBAT content of the original film and MPs were nearly identical (71.6 and 70.6%, respectively) and NPs possessed a 12% lower PBAT content (62.2%; Fig. 7a, c). These results demonstrate that the size-reduced starch was readily leached away from MPs and NPs, while the slight loss of PBAT upon formation of NPs is due to both leaching away of lower-molecular weight polymers and the formation of a gel-like material, noted by the increase of mass remaining at 600 °C (Fig. 7a, c). FTIR analysis also reflected the reduction of starch content upon size reduction, the occurrence of hydrolysis and the absence of oxidation-reduction reactions on the surface (e.g., the absence of cross-link formation or new functional surface groups; discussed in Supplementary Materials).

4. Conclusions

In this study, a simple and effective size reduction process was developed to prepare MPs and NPs from prominent agricultural plastics, PBAT-rich biodegradable mulch films and LDPE, that are likely to represent MPs and NPs occurring in agricultural soils, in contrast to monodisperse polystyrene beads and other commonly employed model materials in fundamental studies. The protocol consisted of cryogenic treatment (to mimic the embrittlement caused by environmental weathering), followed by mechanical milling (to prepare MPs of nominal sizes 45 μm, 106 μm, 250 μm and 840 μm, mimicking the impact of cutting and high-impact mechanical degradation that occur during tillage of plastics into soil). The 106 μm MP fraction was subjected to wet grinding, a process that mimics low-impact shear as would occur between MPs and soil particulates or water (Ravishankar et al., 2018), to produce NPs. The latter's size distribution was bimodal, with the average size of the two populations being 15- and 150-fold smaller than the original 106 μm MP fraction. The size distribution of MPs and the two NP subpopulations was described effectively by the two-parameter Weibull function, and the former was quite broad. Degradation occurred at locally weaker regions possessing lower crystallinity and average molecular weight, and was assisted by the leaching away of polar and lower molecular weight components, such as starch from the PBAT-rich film. The procedure described herein can be applied to several plastic materials, including residual plastic film fragments or debris, to form representative terrestrial MP and NPs materials for future environmental studies, such as ecotoxicity screening and the transport and fate of MPs and NPs in soil ecosystems. The methodology described herein can be employed to investigate the formation of MPs and NPs, such as the kinetics and time course of size reduction, the effect of environmental parameters such as temperature, salinity or the presence of soil particulates.

Acknowledgments

Financial support for this research was provided by the seed grant program of the Institute for a Secure and Sustainable Environment (ISSE) of the University of Tennessee (UT), the USDA Specialty Crops Research Initiative, Coordinated Agricultural Project (Award 2014-51181-22382), and the UT Institute of Agriculture. Ms. Galina Melnichenko and Ms. Marife Anunciado assisted with the collection of GPC data. Dr. David Harper provided technical assistance. We are grateful to BioBag Americas, Inc. (Dunevin, FL, USA) for their kind donation of BioAgri biodegradable mulch film, serving as the source of PBAT.

Funding sources

University of Tennessee (Institute for a Secure and Sustainable Environment), US Department of Agriculture (grant numbers and further information given in the Acknowledgements section).

Appendix A. Supplementary data

Supplementary data to this article can be found online at https://doi.org/10.1016/j.scitotenv.2019.06.241.

References

Alimi, O.S., Farner Budarz, J., Hernandez, L.M., Tufenkji, N., 2018. Microplastics and nanoplastics in aquatic environments: aggregation, deposition, and enhanced contaminant transport. Environ. Sci. Technol. 52, 1704–1724.
Allen, P.A., Michael, N.A., D'Arcy, M., Roda-Boluda, D.C., Whittaker, A.C., Duller, R.A., Armitage, J.J., 2015. Fractionation of grain size in terrestrial sediment routing systems. Basin Res. 29, 180–202.
Bayat, H., Rastgo, M., Mansouri Zadeh, M., Vereecken, H., 2015. Particle size distribution models, their characteristics and fitting capability. J. Hydrol. 529, 872–889.
Bläsing, M., Amelung, W., 2018. Plastics in soil: analytical methods and possible sources. Sci. Total Environ. 612, 422–435.
Bouwmeester, H., Hollman, P.C.H., Peters, R.J.B., 2015. Potential health impact of environmentally released micro- and nanoplastics in the human food production chain: experiences from nanotoxicology. Environ. Sci. Technol. 49, 8932–8947.
Corradini, F., Bartholomeus, H., Huerta Lwanga, E., Gertsen, H., Geissen, V., 2019. Predicting soil microplastic concentration using vis-NIR spectroscopy. Sci. Total Environ. 650, 922–932.
de Souza Machado, A.A., Kloas, W., Zarfl, C., Hempel, S., Rillig, M.C., 2017. Microplastics as an emerging threat to terrestrial ecosystems. Glob. Chang. Biol. 24, 1405–1416.
Domoradzki, M., Korpal, W., 2005. Seed size dependent germination of selected vegetables. Acta Agrophysica 5, 607–612.
Dümichen, E., Barthel, A.-K., Braun, U., Bannick, C.G., Brand, K., Jekel, M., Senz, R., 2015. Analysis of polyethylene microplastics in environmental samples, using a thermal decomposition method. Water Res. 85, 451–457.
Dunbar, C.A., Hickey, A.J., 2000. Evaluation of probability density functions to approximate particle size distributions of representative pharamaceutical aerosols. J. Aerosol Sci. 31, 813–831.
Eckert, E.M., Di Cesare, A., Kettner, M.T., Arias-Andres, M., Fontaneto, D., Grossart, H.-P., Corno, G., 2018. Microplastics increase impact of treated wastewater on freshwater microbial community. Environ. Pollut. 234, 495–502.
EFSA Panel on Contaminants in the Food Chain, 2016. Presence of microplastics and nanoplastics in food, with particular focus on seafood. EFSA J. 14, 4501.
Eitzen, L., Paul, S., Braun, U., Altmann, K., Jekel, M., Ruhl, A.S., 2019. The challenge in preparing particle suspensions for aquatic microplastic research. Environ. Res. 168, 490–495.
Elkharraz, K., Dashevsky, A., Bodmeier, R., 2003. Microparticles prepared by grinding of polymeric films. J. Microencapsul. 20, 661–673. https://doi.org/10.3109/02652040309178354.
Esmaeelnejad, L., Siavashi, F., Seyedmohammadi, J., Shabanpour, M., 2016. The best mathematical models describing particle size distribution of soils. Model. Earth Syst. Environ. 2, 1–11.
Fang, Z., Patterson, B.R., Turner, M.E., 1993. Modeling particle size distributions by the Weibull distribution function. Mater. Charact. 31, 177–182.
Gigault, J., Halle, A.t., Baudrimont, M., Pascal, P.-Y., Gauffre, F., Phi, T.-L., El Hadri, H., Grassl, B., Reynaud, S., 2018. Current opinion: what is a nanoplastic? Environ. Pollut. 235, 1030–1034.

Goedecke, C., Mülow-Stollin, U., Hering, S., Richter, J., Piechotta, C., Paul, A., Braun, U., 2017. A first pilot study on the sorption of environmental pollutants on various microplastic materials. J. Environ. Anal. Chem 4, 191.
Guo, X., Pang, J., Chen, S., Jia, H., 2018. Sorption properties of tylosin on four different microplastics. Chemosphere 209, 240–245.
Hartmann, N.B., et al., 2019. Are we speaking the same language? Recommendations for a definition and categorization framework for plastic debris. Environ. Sci. Technol 53, 1039–1047.
Hayes, D.G., Wadsworth, L.C., Sintim, H.Y., Flury, M., English, M., Schaeffer, S., Saxton, A.M., 2017. Effect of diverse weathering conditions on the physicochemical properties of biodegradable plastic mulches. Polym. Testing. 62, 454–467.
Hayes, D.G., et al., 2019. Biodegradable plastic mulch films for sustainable specialty crop production. In: Gutierrez, T.J. (Ed.), Polymers for Agri-Food Applications. Springer Nature, Berlin (in press).
Horton, A.A., Walton, A., Spurgeon, D.J., Lahive, E., Svendsen, C., 2017. Microplastics in freshwater and terrestrial environments: evaluating the current understanding to identify the knowledge gaps and future research priorities. Sci. Total Environ. 586, 127–141.
Huerta Lwanga, E., Gertsen, H., Gooren, H., Peters, P., Salánki, T., van der Ploeg, M., Besseling, E., Koelmans, A.A., Geissen, V., 2017. Incorporation of microplastics from litter into burrows of *Lumbricus terrestris*. Environ. Pollut. 220, 523–531.
Hussain, I., Hamid, H., 2003. Plastics in agriculture. In: Andrady, A.L. (Ed.), Plastics and the Environment. John Wiley and Sons, New York, pp. 185–209.
Jambeck, J.R., Geyer, R., Wilcox, C., Siegler, T.R., Perryman, M., Andrady, A., Narayan, R., Law, K.L., 2015. Plastic waste inputs from land into the ocean. Science 347, 768.
Jonna, S., Lyons, J., 2005. Processing and properties of cryogenically milled post-consumer mixed plastic waste. Polym. Testing. 24, 428–434.
Kasirajan, S., Ngouajio, M., 2012. Polyethylene and biodegradable mulches for agricultural applications: a review. Agron. Sustain. Dev. 32, 501–529.
Koelmans, A.A., Besseling, E., Wegner, A., Foekema, E.M., 2013. Plastic as a carrier of POPs to aquatic organisms: a model analysis. Environ Sci Technol 47.
Kühn, S., van Oyen, A., Booth, A.M., Meijboom, A., van Franeker, J.A., 2018. Marine microplastic: preparation of relevant test materials for laboratory assessment of ecosystem impacts. Chemosphere 213, 103–113.
Lu, L., Wan, Z., Luo, T., Fu, Z., Jin, Y., 2018. Polystyrene microplastics induce gut microbiota dysbiosis and hepatic lipid metabolism disorder in mice. Sci. Total Environ. 631-632, 449–458.
Lynch, A.J., Rowland, C.A., 2005. The History of Grinding. Society for Mining, Metallurgy, and Exploration, Inc., Littleton, CO, USA.
Mattsson, K., Hansson, L.A., Cedervall, T., 2015. Nano-plastics in the aquatic environment. Environ. Sci.: Processes Impacts. 17, 1712–1721.
McCormick, A., Hoellein, T.J., Mason, S.A., Schluep, J., Kelly, J.J., 2014. Microplastic is an abundant and distinct microbial habitat in an urban river. Environ. Sci. Technol. 48, 11863–11871.
Miles, C., DeVetter, L., Ghimire, S., Hayes, D., G., 2017. Suitability of biodegradable plastic mulches for organic and sustainable agricultural production systems. HortSci. 52, 10–15.
Ng, E.-L., Huerta Lwanga, E., Eldridge, S.M., Johnston, P., Hu, H.-W., Geissen, V., Chen, D., 2018. An overview of microplastic and nanoplastic pollution in agroecosystems. Sci. Total Environ. 627, 1377–1388.
Nizzetto, L., Futter, M., Langaas, S., 2016. Are agricultural soils dumps for microplastics of urban origin? Environ. Sci. Technol. 50, 10777–10779.
Oberbeckmann, S., Kreikemeyer, B., Labrenz, M., 2018. Environmental factors support the formation of specific bacterial assemblages on microplastics. Front. Microbiol. 8, 2709.
Poulose, A.M., Piccarolo, S., Carbone, D., Al-Zahrani, S.M., 2016. Influence of plasticizers and cryogenic grinding on the high-cooling-rate solidification behavior of PBT/PET blends. J. Appl. Polym. Sci. 133, 43083.
Ravishankar, K., Ramesh, P.S., Sadhasivam, B., Raghavachari, D., 2018. Wear-induced mechanical degradation of plastics by low-energy wet-grinding. Polym. Degr. Stab. 158, 212–219.
Robotti, M., Dosta, S., Cano, I.G., Concustell, A., Cinca, N., Guilemany, J.M., 2016. Attrition and cryogenic milling powder production for low pressure cold gas spray and composite coatings characterization. Adv. Powder Technol. 27, 1257–1264.
Saba, N., Tahir, P.M., Abdan, K., Ibrahim, N.A., 2015. Preparation and characterization of fire retardant nanofiller from oil palm empty fruit bunch fibers. BioResources 10, 4530–4543.
Scarascia-Mugnozza, G., Sica, C., Russo, G., 2011. Plastic materials in European agriculture: actual use and perspectives. J. Agric. Eng 42, 15–28.
Scheurer, M., Bigalke, M., 2018. Microplastics in Swiss floodplain soils. Environ. Sci. Technol. 52, 3591–3598.
Schmidt, J., Plata, M., Tröger, S., Peukert, W., 2012. Production of polymer particles below 5μm by wet grinding. Powder Technol. 228, 84–90.
Schmidt, J., Romeis, S., Peukert, W., 2017. Production of PBT/PC particle systems by wet grinding. AIP Conf. Proc. 1914, 050003.
Schneider, C.A., Rasband, W.S., Eliceiri, K.W., 2012. NIH image to ImageJ: 25 years of image analysis. Nature Meth 9, 671.
Schwabl, P., Liebmann, B., Köppel, S., Königshofer, P., Bucsics, T., Trauner, M., Reiberger, T., 2018. Assessment of Microplastics Concentrations in Human Stool: Preliminary Results (United Eurpean Gastroenterology Conference, Vienna, Austria, 20–24 October 2018). vol. 2019.
Seguro, J.V., Lambert, T.W., 2000. Modern estimation of the parameters of the Weibull wind speed distribution for wind energy analysis. J. Wind Eng. Ind. Aerodyn. 85, 75–84.
Steinmetz, Z., Wollmann, C., Schaefer, M., Buchmann, C., David, J., Tröger, J., Muñoz, K., Frör, O., Schaumann, G.E., 2016. Plastic mulching in agriculture. Trading short-term agronomic benefits for long-term soil degradation? Sci. Total Environ. 550, 690–705.
Varga, E.G., Titchener-Hooker, N.J., Dunnill, P., 2001. Prediction of the pilot-scale recovery of a recombinant yeast enzyme using integrated models. Biotechnol. Bioeng. 74, 96–107.
von Moos, N., Burkhardt-Holm, P., Kohler, A., 2012. Uptake and effects of microplastics on cells and tissue of the blue mussel *Mytilus edulis* L. after an experimental exposure. Environ. Sci. Technol. 46.
Watano, S., Matsuo, M., Nakamura, H., Miyazaki, T., 2015. Improvement of dissolution rate of poorly water-soluble drug by wet grinding with bio-compatible phospholipid polymer. Chem. Eng. Sci. 125, 25–31.
Wilczek, M., Bertling, J., Hintemann, D., 2004. Optimised technologies for cryogenic grinding. Int. J. Mineral Proc. 74, S425–S434.
Wright, S.L., Kelly, F.J., 2017. Plastic and human health: a micro issue? Environ. Sci. Technol. 51, 6634–6647.
Xu, B., Liu, F., Brookes, P.C., Xu, J., 2018. Microplastics play a minor role in tetracycline sorption in the presence of dissolved organic matter. Environ. Pollut. 240, 87–94.
Young, T.M., León, R.V., Chen, C.-H., Chen, W., Guess, F.M., Edwards, D.J., 2015. Robustly estimating lower percentiles when observations are costly. Quality Eng 27, 361–373.
Zhang, Y., Fei, S., Yu, M., Guo, Y., He, H., Zhang, Y., Yin, T., Xu, H., Tang, X., 2018. Injectable sustained release PLA microparticles prepared by solvent evaporation-media milling technology. Drug Dev. Ind. Pharm. 44, 1591–1597.
Zhu, D., Chen, Q.-L., An, X.-L., Yang, X.-R., Christie, P., Ke, X., Wu, L.-H., Zhu, Y.-G., 2018. Exposure of soil collembolans to microplastics perturbs their gut microbiota and alters their isotopic composition. Soil Biol. Biochem. 116, 302–310.
Zuo, L.-Z., Li, H.-X., Lin, L., Sun, Y.-X., Diao, Z.-H., Liu, S., Zhang, Z.-Y., Xu, X.-R., 2019. Sorption and desorption of phenanthrene on biodegradable poly(butylene adipate co-terephtalate) microplastics. Chemosphere 215, 25–32.